Tunable luminescent properties of Dy^{3+}, Tm^{3+} doped Li_2CaSiO_4 phosphors for near-UV light-emitting diodes

WENKE RUAN, MUBIAO XIE*, JIATING QIU, YIWEI XIAN, XIACHAN ZHANG
School of Chemistry and Chemical Engineering, Insitute for Advanced Materials, Lingnan Normal University, Zhanjiang 524048, China

A series of Dy^{3+}-Tm^{3+} co-activated Li_2CaSiO_4 phosphors were synthesized by a high temperature solid-state reaction and characterized using X-ray powder diffraction as well as luminescence spectroscopy. The excitation and emission spectra show that all the Tm^{3+} and Dy^{3+} co-doped Li_2CaSiO_4 samples can be effectively excited by UV light and then emit light in the region between blue and white. Furthermore, the color coordinate of as-obtained samples exited at 360 nm were able to be adjusted from warm-white to cold-white light area by varying the doping concentrations of Tm^{3+} and Dy^{3+}. Hence, Li_2CaSiO_4:Dy^{3+}, Tm^{3+} phosphors have potential application as UV-convertible phosphor for near-UV excited white light-emitting diodes.

(Received February 17, 2023; accepted August 7, 2023)

Keywords: Phosphor, Luminescence, LEDs, Li_2CaSiO_4, Tm^{3+}, Dy^{3+}

1. Introduction

In recent years, White-Light-Emitting-Diode (wLED) has been widely recognized as the fourth-generation lighting source after the incandescent lamp, fluorescent lamp, and high-pressure gas discharge lamp due to its advantages of high luminous efficiency, long life, good stability, and energy saving and environmental protection. [1-3]. In white light emitting diodes (LEDs) application, LEDs can be fabricated in three ways: (1) Combine yellow YAG: Ce^{3+} phosphor with a gallium nitride (GaN)-based bluechip; (2) Combine the GaN-based blue chip with green and red phosphors or the ultraviolet (UV) (350–420 nm) chip with blue, green, and red tri-color phosphors; (3) Combine a single-composition white-emitting phosphor with an UV LED[4-6]. Recently, the third type has drawn much attention because of its small color aberration, great color rendering index and lower production cost [7-9]. The previous studies have showed that the single composition white-emitting phosphor can be achieved by co-doping rare-earth ions or transition metal ions into the same host matrix. Hence, many studies recently focused on the Eu^{2+}/Mn^{2+} [10], Ce^{3+}/Mn^{2+} [11], Ce^{3+}/Eu^{2+} [12], and Ce^{3+}/Tb^{3+} [13] couples. However, the Dy^{3+}-doped, Dy^{3+}-Tm^{3+} co-doped phosphors, which can be synthesized more conveniently in an ambient atmosphere, were rarely investigated. It is well known that the Dy^{3+} ion can emit yellow and blue light through the transitions $^4F_{9/2}\rightarrow{}^6H_{13/2}$ and $^4F_{9/2}\rightarrow{}^6H_{15/2}$ by absorbing UV light [14]. That is to say, white light can be generated by single Dy^{3+} ion when the ratio of the yellow light and blue light are properly adjusted. Unfortunately, it is hard to adjust a proper yellow/blue ratio to generate a suitable white light in single Dy^{3+}-doping system [15]. This phenomenon usually makes the color temperature of the white-light emission generated by Dy^{3+} ion not suitable. The Tm^{3+} ion can generate blue light through the $^1G_4\rightarrow{}^3H_6$ transition which can compensate the blue light generated by Dy^{3+} ions. Therefore, white-light emission might be generated by co-doping appropriate amounts of Dy^{3+} and Tm^{3+} in the specific host [16-18].

The silicate-matrix is an excellent luminescent host because of its good chemical and thermal stability. Recently, luminescence properties of Eu^{3+}, Eu^{2+} and Ce^{3+} doped Li_2CaSiO_4 have been reported for the LEDs application [19-23]. Dy^{3+}-doped Li_2CaSiO_4 phosphors have been observed for their potential application for near-UV excited WLEDs [24]. In the present work, we obtained white-light-emitting phosphors by co-doping Tm^{3+}-Dy^{3+} in a single host.

2. Experimental section

A series of samples Li_2CaSiO_4:$0.06Dy^{3+}$, Li_2CaSiO_4:$0.06Tm^{3+}$, Li_2CaSiO_4:$0.06Dy^{3+}$, $x$$Tm^{3+}$ (x = 0.01, 0.02, 0.04, 0.06, 0.08, 0.10) were prepared by a conventional solid-state reaction technique at high temperature. The reactants include analytical reagent grade Li_2CO_3, $CaCO_3$, SiO_2 and rare earth oxides (Tm_2O_3, 99.99%; Dy_2O_3, 99.99%). Appropriate amount of starting materials were grounded in an agate mortar and heated in

air at 1073K for six hours. The final products were cooled down to room temperature (RT) and grounded again into a white powder.

The phase purity was characterized by a powder X-ray diffraction (XRD) analyzed using Cu Kα radiation (λ = 1.5405 Å, 40 kV, 30 mA) on a Rigaku D/max 2200 vpc X-Ray Diffractometer at room temperature (RT). The photoluminescence spectra at RT were recorded on an FLS1000 spectrometer. A 350W xenon lamp was used as the excitation source.

3. Results and discussion

3.1. XRD measurement

Powder XRD measurements were performed for all final samples to check the phase purity and the phase structure. The XRD patterns of samples Li_2CaSiO_4:0.06 Dy^{3+}, Li_2CaSiO_4:0.06 Tm^{3+}, Li_2CaSiO_4:0.06Dy^{3+},0.06 Tm^{3+} is shown in Fig. 1(a). It can be seen that that the XRD patterns of the sample matches well with the JCPDS card (27-0290) [Li_2CaSiO_4], indicating that doping of Dy^{3+}, Tm^{3+} ions does not cause significant change in the host structure. Some impurities with small peaks were identified as (*Ca_2SiO_4 (JCPDS#33-0302), which may be caused by insufficient precursor reactions. Clearly, a small amount of phase change would not significantly affect our analysis. In order to further study the crystal structure of Li_2CaSiO_4, combined with the work of Gard [25], it is found that the crystal structure of Li_2CaSiO_4 is a body-centered tetragonal system, and the spatial parameters are a = (0.504 7±0.000 5 Å), c = (0.648 6±0.000 6 Å), the space group is $I\bar{4}2m$. In the Li_2CaSiO_4 unit cell, there is only one octa-coordinated strongly distorted dodecahedral calcium site. There are two kinds of Ca-O bonds in the crystal lattice, which four Ca-O bonds have a bond length of 0.269 nm, and the other four The bond length of the Ca-O bond is 0.241 nm. In addition, by observing the illustration on the right of Fig. 1(b), it can be found that the diffraction peaks of the crystal plane between 2θ = 35° - 40° shift to a large angle direction after doping with Dy^{3+} and Tm^{3+} ions. According to the Bragg equation $2dsin\theta = n\lambda$, the main reason for this peak shift is due to the small radius Dy^{3+} (R_{Dy}^{3+} = 0.091 nm, CN = 8), Tm^{3+} (R_{Tm}^{3+} = 0.088 nm, CN = 8) displacement formula instead of Ca^{2+} with a larger radius (R_{Ca}^{2+} = 0.100 nm, CN = 8), the difference in ion radius and charge leads to smaller unit cell parameters [26].

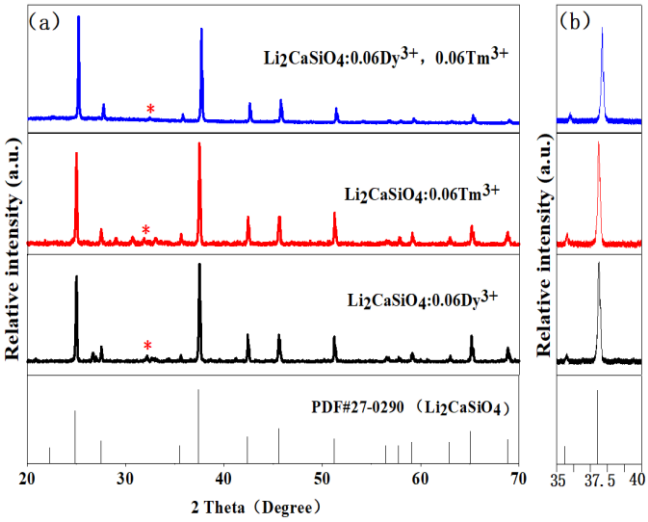

Fig. 1. XRD patterns (a) and located between 2θ = 35° - 40° diffraction peak position offset (b) of Li_2CaSiO_4:0.06Dy^{3+}, Li_2CaSiO_4:0.06Tm^{3+}, $Li_2CaSiO4$:0.06Dy^{3+},0.06Tm^{3+} phosphors (color online)

3.2. Dy^{3+} luminescence in Li_2CaSiO_4

Fig. 2 shows the excitation spectrum (curve a) and the emission spectrum (curve b) of the single Dy^{3+} -doped phosphor Li_2CaSiO_4:0.06Dy^{3+}. Curve a is the excitation spectrum in the range 250-500 nm by monitoring the emission of Dy^{3+} at 575 nm. The excitation spectrum consists of a series of absorption lines, in which the peak at ~350 nm is dominant. This intense excitation peak is assigned to $^6H_{15/2}\rightarrow{}^4P_{7/2}$ transition of Dy^{3+} ion. Other peaks at ~325 nm, ~365 m and ~386 nm are ascribed to the transitions $^6H_{15/2}\rightarrow{}^4M_{17/2}$, $^6H_{15/2}\rightarrow{}^4P_{3/2}$, and $^6H_{15/2}\rightarrow{}^4F_{7/2}$ of Dy^{3+} ion, respectively. The emission spectrum of Li_2CaSiO_4:0.06Dy^{3+} under 350 nm excitation is shown in Fig. 2(b). There are two group emission peaks in the wavelength range 450-600 nm. The blue peak (~ 490 nm) corresponds to the $^4F_{9/2}\rightarrow{}^6H_{15/2}$ transition and the yellow peak (~579 nm) corresponds with the $^4F_{9/2}\rightarrow{}^6H_{13/2}$ transition of Dy^{3+}. The intensities of the blue and yellow peaks are nearly the same, indicating that white light can be obtained in the prepared phosphor Li_2CaSiO_4:0.06Dy^{3+}. The chromaticity coordinates (x, y) of Li_2CaSiO_4:0.06Dy^{3+} are calculated to be (0.348, 0.375), indicating that the present phosphor Li_2CaSiO_4:0.06Dy^{3+} is located in yellow-white light region. As a white-light emission phosphor for LEDs lamp, the emission color is closed to the standard white-light point (0.33, 0.33), but still has a little deviation.

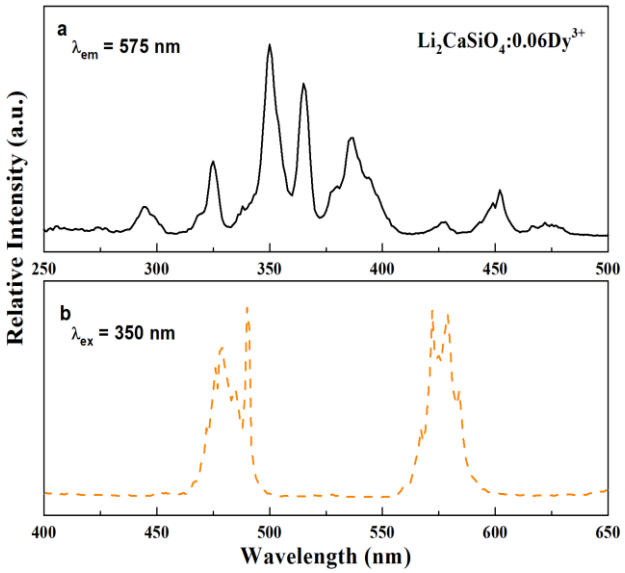

Fig. 2. The excitation (curve a, λ_{em} = 575 nm) and emission (curve b, λ_{ex} = 350 nm) of sample Li_2CaSiO_4:0.06Dy^{3+}

3.3. Tm^{3+} luminescence in Li_2CaSiO_4

The excitation spectrum (curve a, λ_{em} = 457 nm) and the emission spectra (curve b, λ_{ex} = 354 nm) of sample Li_2CaSiO_4:0.06Tm^{3+} are shown in Fig. 3. The excitation spectrum presents one strong peak centered at ~354 nm in 340–370 nm range by monitoring emission at 457 nm, which is assigned to the $^3H_6 \rightarrow {}^1D_2$ electronic transition of Tm^{3+} ions. The emission spectra under 354 nm excitation are displayed in curves b of Fig. 3. The emission curve consist of an emission peak at about 452 nm in the wavelength range 400-550 nm, corresponding to the $^1D_2 \rightarrow {}^3F_4$ transition of Tm^{3+} ions.

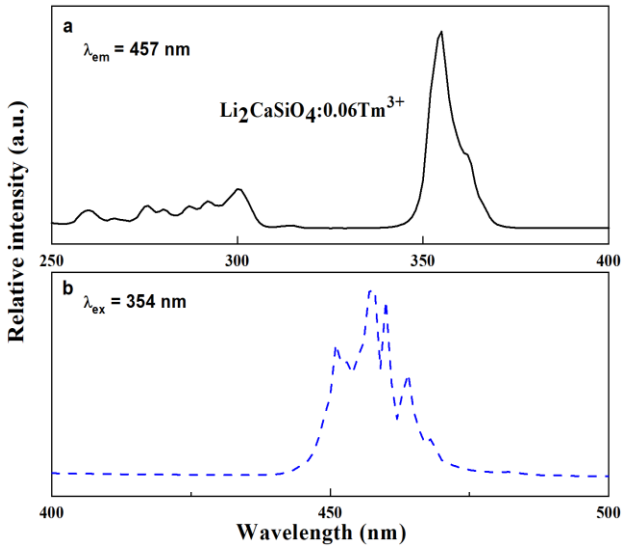

Fig. 3. The excitation (curve a, λ_{em} = 457 nm) and emission (curve b, λ_{ex} = 354 nm) of sample Li_2CaSiO_4: 0.06Tm^{3+}

3.4. Tm^{3+}-Dy^{3+} luminescence in Li_2CaSiO_4

Fig. 4 presents the emission spectra of Tm^{3+}-Dy^{3+} co-doped samples Li_2CaSiO_4:0.06Dy^{3+}, $x$$Tm^{3+}$ with various contents of Tm^{3+} under the UV light (360 nm) excitation, and the amplified emission peaks in the wavelength range from 445 to 470 nm is presented in the inset of Fig. 4. With increasing concentration of Tm^{3+} increasing, a different trend for the luminescence intensity can be seen. Fig. 5 shows the dependence of the intensities of the Tm^{3+} $^1D_2 \rightarrow {}^3F_4$ transition at 451 nm and the $^4F_{9/2} \rightarrow {}^6H_{15/2}$ (477 nm), $^4F_{9/2} \rightarrow {}^6H_{13/2}$ (570 nm) transitions of Dy^{3+} as a function of Tm^{3+} concentrations, respectively. With doping concentration increasing of Tm^{3+} in the Tm^{3+}-Dy^{3+} co-doped system, the intensities of Tm^{3+} $^1D_2 \rightarrow {}^3F_4$ transition increase linearly, and reach a maximum at the concentration x = 0.06, while that of Dy^{3+} decreases gradually. It is possibly due to the quenching effect of Tm^{3+} on the emission intensity of Dy^{3+}.

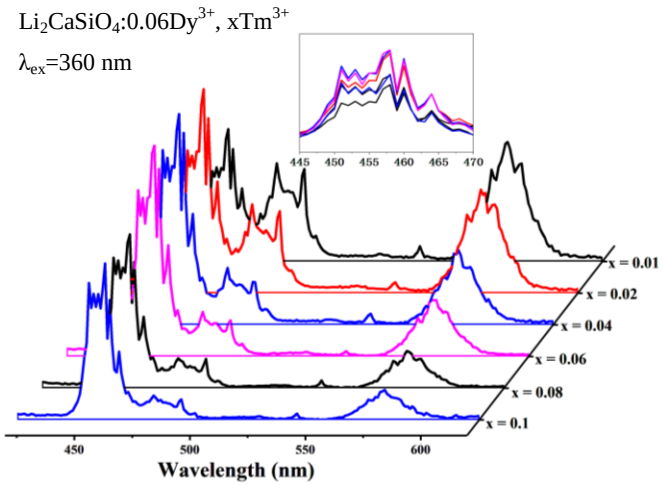

Fig. 4. Emission spectra of samples Li_2CaSiO_4: 0.06Dy^{3+}, xTm^{3+} (x = 0.01, 0.02, 0.04, 0.06, 0.08, 0.10) (color online)

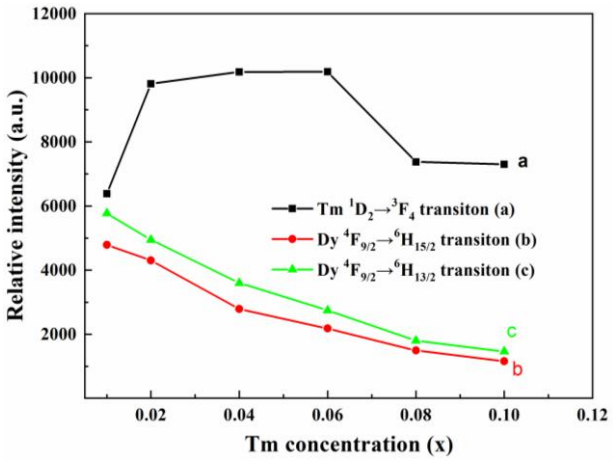

Fig. 5. The dependence of the intensities of the Tm^{3+} $^1D_2 \rightarrow {}^3F_4$ transition (a) and the $^4F_{9/2} \rightarrow {}^6H_{15/2}$(b), $^4F_{9/2} \rightarrow {}^6H_{13/2}$ (c) transitions of Dy^{3+} as a function of Tm^{3+} concentrations (color online)

In order to further analyze the mechanism of concentration quenching, Blasse [27] pointed out that the critical distance R_c of luminescent ion concentration quenching can be obtained by formula (1).

$$R_c = 2\left(\frac{3V}{4\pi X_c N}\right)^{1/3} \quad (1)$$

In the formula: V is the unit cell volume, N is the number of atoms contained in the unit cell, and X_c is the critical concentration of doped ions. For Li_2CaSiO_4, V = 165.21Å, X_c = 0.06, N = 2 [23]. Therefore, Rc can be calculated to be about 13.8Å. Blasse [28] believes that if R_c is greater than 5Å, the electric multipole moment interaction is the mechanism of concentration quenching, otherwise it is the electron cloud exchange. In this system, Rc is much greater than 5Å, so the mechanism of concentration quenching is electric multipole moment interaction.The type of electric multipole moment interaction can be determined by equation (2) [29].

$$\frac{I}{x} = \left[1+\beta(x)^{\theta/3}\right]^{-1} \quad (2)$$

In the formula: x is the concentration of activator, I is the integrated intensity of luminescence, θ = 6, 8, 10 are electric dipole moment-electric dipole moment, electric dipole moment-electric quadrupole moment, electric quadrupole moment-electric quadrupole moment. For the same material, $\beta(x)$ is a constant. Make the relationship curve between $\log(I/x(Tm^{3+}))$ and $\log(x(Tm^{3+}))$ (Fig. 6), and get the slope of (θ/3 = -0.849). Therefore, the value of θ is about 2.5. Combining the results of Formula (1) and Formula (2), it shows that the concentration quenching mechanism of Tm^{3+} in Li_2CaSiO_4:Dy^{3+}, Tm^{3+} phosphors is mainly the electric dipole moment-electric dipole moment interaction.

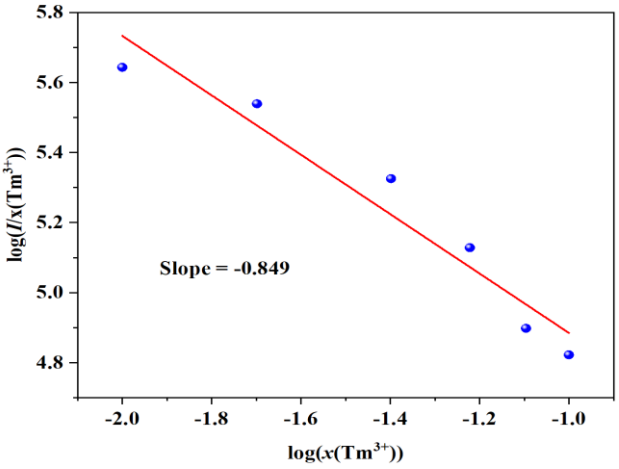

Fig. 6. Li_2CaSiO_4:Dy^{3+}, Tm^{3+} relationship curve of $log(I/x(Tm^{3+}))$-$log(x(Tm^{3+})$

Table 1. Luminous characteristic parameters and CIE chromaticity coordinates for Li_2CaSiO_4:0.06Dy^{3+}; Li_2CaSiO_4:0.06Tm^{3+}; Li_2CaSiO_4:0.06Dy^{3+}, xTm^{3+} upon excitation at 360 nm

Samples Number	Tm concentration (x)	Emission peak positions/nm	Emission intensity a.u.	Chromaticity coordinates (λ_{ex} = 360 nm)
a	Li_2CaSiO_4:0.06Dy^{3+}	575 nm	8523	(0.335,0.407)
b	0.01	458 nm	6420	(0.294,0.270)
c	0.02	458 nm	9870	(0.266,0.224)
d	0.04	458 nm	10210	(0.252,0.200)
e	0.06	458 nm	10240	(0.244,0.184)
f	0.08	458 nm	7456	(0.233,0.166)
g	0.10	458 nm	7576	(0.225,0.159)
h	Li_2CaSiO_4:0.06Tm^{3+}	457 nm	248800	(0.164,0.121)

The corresponding chromaticity diagram for these eight samples Li_2CaSiO_4:0.06Dy^{3+}; Li_2CaSiO_4:0.06Tm^{3+}; Li_2CaSiO_4: 0.06Dy^{3+}, xTm^{3+}(x = 0.01, 0.02, 0.04, 0.06, 0.08, 0.10) are presented in Fig. 7 and Table 1. The color coordinates of the sample Li_2CaSiO_4: 0.06Dy^{3+}, 0.01Tm^{3+} is x = 0.294, y = 0.270, which is locates at the white-light region. With the Tm^{3+} concentration increasing, the color coordinates of the samples decline in line, and finally to the blue region, implying that the concentration of Tm^{3+} has great influence in the tuning of color coordinate for Li_2CaSiO_4: Tm^{3+}, Dy^{3+} phosphors.

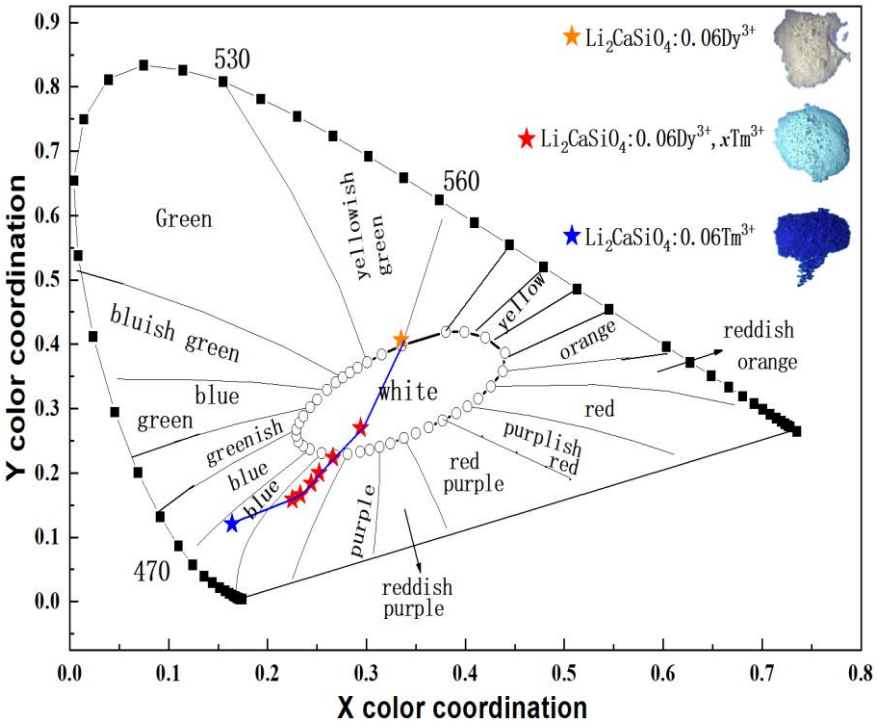

Fig. 7. The chromaticity coordinate diagram Dy^{3+}- and Tm^{3+}-doped Li_2CaSiO_4 under 360 nm excitation. The digital images of the phosphors under 365 nm excitation are shown in the inset (color online)

4. Conclusions

The luminescence properties of Dy^{3+}-doped phosphors Li_2CaSiO_4:Dy^{3+}, Tm^{3+} -doped phosphors Li_2CaSiO_4:Tm^{3+} and Tm^{3+}-Dy^{3+} co-doped phosphors Li_2CaSiO_4: Tm^{3+}-Dy^{3+} were investigated. Li_2CaSiO_4:Tm^{3+} and Li_2CaSiO_4:Dy^{3+} phosphors can absorb UV light, and emit blue and white light, respectively. For co-doped samples phosphors Li_2CaSiO_4:0.06Dy^{3+}, $x$$Tm^{3+}$, the color temperate can be tuned from yellow-white to blue-white light area by varying the concentrations of Tm^{3+} ions. Thus, the as-fabricated single-composition Li_2CaSiO_4:Tm^{3+},Dy^{3+} phosphor are promising candidates for white light emitting diodes.

Acknowledgment

The work is financially supported by Guangdong Basic and Applied Basic Research Foundation (2022A1515012586), Zhanjiang Science and Technology Plan Project (2022A01027), Lingnan Normal University School Project (LY2205) and the Open Project of Key Laboratory of Chean Energy Material Chemistry in Guangdong General University (CEMC2022007).

References

[1] G. G. Li, Y. Tian, Y. Zhao, Jun. Lin, Chem. Soc. Rev. **44**, 8688 (2015).
[2] J. F. Sun, X. Y. Zhang, R. Zhang, Mater. Lett. **267**, 127559 (2020).
[3] L. L. Devi, C. K. Jayasankar, J. Lumin. **221**, 116996 (2020).
[4] X. Y. Fan, J. Y. Si, M. J. Xu, G. H. Li, J. M. Tang, G. M. Cai, Ceram. Int. **47**, 12056 (2021).
[5] M. B. Xie, G. X. Zhu, R. K. Pan, D. Y. Li, D. J. Hou, J. Phys. D Appl. Phys. **49**, 225105 (2016).
[6] J. Y. Wang, J. B. Wang, P. Duan, J. Lumin. **145**, 1 (2014).
[7] S. H. Pan, K. P. Liu, Z. T. Ling, K. P. Guo, S. L. Wang, M. Y. Chen, C. F. Si, Z. Y. Tang, B. Wei, Surf. Coat. Tech. **363**, 442 (2019).
[8] Y. P. Manwar, R. S. Palaspagar, R. P. Sonekar, S. K. Omanwar, J. Mater. Sci.-Mater. El. **28**, 994 (2017).
[9] R. Xiang, X. J. Liang, Q. Y. Xi, Z. F. Yuan, C. R. Chen, W. D. Xiang, Ceram. Int. **16**, 19276 (2016).
[10] R. T. Bao, S. Jin, D. M. Liu, C. Wen, J. L. Shi, Z. P. Wang, X. X. Yuan, P. L. Li, Z. P. Yang, Z. J. Wang, Optik **5**, 166450 (2021).
[11] L. Kang, H. W. Wang, X. S. Li, J. C. Zhou, J. Alloys Compd. **859**, 1 (2021).
[12] T. T. Wu, F. L. Meng, Y. Du, Y. N. Tian, J. Ma, Z. H. Bai, X. Y. Zhang, J. Mater. Sci.-Mater. El. **28**, 10645 (2017).

[13] S. Shweta, B. Nameeta, D. P Bisen, D. Pradeep, G. Ritu, Opt. Laser. Technol. **135**, 106682 (2021).
[14] C. R. Kesavulu, C. K. Jayasankar, Mater. Chem. Phys. **130**, 1078 (2011).
[15] Y. Z. Yin, C. Dou, Z. Wang, J. H. Li, J. Gao, S. J. Sun, B. Teng, Y. Che, S. Ullah, D. G. Zhong, Optik **231**, 166430 (2021).
[16] L. Li, M. W. Dou, Y. L. Yan, Y. H. Li, F. L. Ling, S. Jiang, G. T. Xiang, J. Liu, X. J. Zhou, Opt. Mater. **102**, 109808 (2020).
[17] M. H. Fan, S. Liu, K. Yang, J. Guo, J. X. Wang, X. H. Wang, Q. Liu, B. Wei, Ceram. Int. **46**, 6926 (2020).
[18] P. H. Yang, X. Yu, X. H. Xu, T. M. Jiang, H. L. Yu, D. C. Zhou, Z. W. Yang, Z. G. Song, J. B. Qiu, J. Solid State Chem. **202**, 143 (2013).
[19] L. H. Zhou, P. Du, L. Li, Sci. Rep. **10**, 20180 (2020).
[20] S. Z. Liao, W. L. Zhang, J. L. Zhang, Ceram. Int. **44**, 18413 (2018).
[21] L. Chen, A. Q. Luo, Y. Zhang, F. Y. Liu, Y. Jiang, Q. S. Xu, X. H. Chen, Q. Z. Hu, S. F. Chen, K. J. Chen, H. C. Kuo, ACS Comb. Sci. **14**, 636 (2012).
[22] J. M. Zhong, W. R. Zhao, L. C. Lan, J. Q. Wang, J. H. Chen, N. H. Wang, J. Alloys Compd. **15**, 213 (2014).
[23] M. B. Xie, T. J. Song, ECS J. Solid State Sci. Technol. **2**, 29 (2013).
[24] E. Erdoğmuş, J. Appl. Spectrosc. **83**, 212 (2016).
[25] J. A. Gard, A. R. West, J. Solid State Chem. **7**, 422 (1973).
[26] R. D. Shannon, Acta Cryst. **32**, 751 (1976).
[27] G. Blasse, Phys. Lett. A. **28**, 444 (1968).
[28] D. L. Dexter, J. Chem. Phys. **21**, 836 (1953).
[29] L. G. Van Uitert, J. Electrochem. Soc. **114**, 1048 (1967).

*Corresponding author: xiemubiao@163.com